

# Encapsulation of DNA-Templated Chromophore Assemblies within Virus Protein Nanotubes\*\*

Andrés de la Escosura,\* Pim G. A. Janssen, Albertus P. H. J. Schenning, Roeland J. M. Nolte, and Jeroen J. L. M. Cornelissen\*

The use of biomolecules, which self-assemble to form precise nanostructures, has attracted growing interest in nanotechnology over the last decade.<sup>[1–4]</sup> As an example, DNA has been applied as a platform for the positioning of functional molecules and nanoparticles with geometrical, size, and positional control.<sup>[5–11]</sup> Viruses have also been used as robust and monodisperse scaffolds for the incorporation of chemical entities both in their inner cavities and on their exterior surfaces.<sup>[12–17]</sup> Filamentous viruses such as the Tobacco mosaic virus and M13 viruses can be used to construct one-dimensional arrays, mainly through the attachment of small building blocks to their surfaces.<sup>[18–21]</sup>

Herein, we describe a unique strategy to assemble chromophoric molecules into very long helical stacks by using both types of biological scaffolds outlined above, that is, DNA to template the chromophore assembly<sup>[22–24]</sup> and the Cowpea chlorotic mottle virus (CCMV) protein to create nanotubes that can hold the DNA–chromophore architectures.

CCMV<sup>[25,26]</sup> is an icosahedral virus with an outer diameter of 28 nm and an inner cavity 18 nm in diameter. The capsid shell is formed by 180 coat protein (CP) subunits that assemble with  $T=3$  Caspar–Klug symmetry around a central RNA matrix. The CP consists of 189 amino acids, with nine basic residues at the N-terminal RNA binding domain. At neutral pH and high ionic strength, CCMV virions disassemble *in vitro* into protein dimers. After removal of the RNA, CP dimers can be reassembled to form empty capsids, the size of which varies with the assembly conditions. Furthermore, it has been reported that when double-stranded DNA (dsDNA) is encapsulated at neutral pH and low ionic strength, the CP forms tubular structures 17 nm in diameter.<sup>[27]</sup>

We studied DNA-templated assemblies that consist of a single-stranded DNA (ssDNA) template, that is, oligothymines (T<sub>q</sub>) of various lengths, to which naphthalene (G1), stilbene (G2) and oligo(*p*-phenylenevinylene) (OPV; G3) derivatives are bound by complementary hydrogen bonds. In T<sub>q</sub>–G complexes, one strand is DNA and the other strand is a supramolecular stack of G molecules. Only one strand is negatively charged, instead of two as for dsDNA. The DNA–hybrid complexes normally adopt a right-handed helical arrangement stabilized by  $\pi$ – $\pi$  stacking and hydrophobic interactions between the adjacent guest moieties, with the phosphate groups pointing to the exterior of the backbone. The interplay between the chromophore, DNA template, and protein mantle results in a hierarchical organization of components on different length scales, and the chromophores within the tubes remaining in their helical arrangement (Figure 1).

We have studied the assembly of CP alone and in the presence of T40, G1 and the T40–G1 complex. The concentration of CP was 0.04 mM in all samples. All experiments were carried out in 50 mM Tris–HCl buffer at pH 7.5 and low salt concentration (0.1 M NaCl). The temperature was kept at 5 °C, and 5 equivalents of G1 ( $[G1] = 1$  mM) relative to the thymine units ( $[T]_{T40} = 0.2$  mM;  $[T]_{T40}$  represents the total concentration of repeating thymine units in the assembly sample) were used. These conditions ensure a high degree of binding between G1 and T40 (Figure S1 in the Supporting Information).<sup>[22]</sup> When the nonchiral diaminotriazine-functionalized guest was added to T<sub>q</sub> at low temperatures, an induced bisignate Cotton effect was observed in the guest absorption region (Figure S1a in the Supporting Information). The chirality of the template is expressed in the supramolecular organization of guest molecules, which shows that they bind to T<sub>q</sub>. These binding events result in a rigidification of the ssDNA template, as was shown by cryo-

[\*] Dr. A. de la Escosura,<sup>[†]</sup> Prof. R. J. M. Nolte, Prof. J. J. L. M. Cornelissen<sup>[#]</sup>  
Institute for Molecules and Materials  
Radboud University Nijmegen  
Toernooiveld 1, 6525 ED Nijmegen (The Netherlands)

Dr. P. G. A. Janssen, Dr. A. P. H. J. Schenning  
Laboratory for Macromolecular and Organic Chemistry  
Eindhoven University of Technology  
PO Box 513, 5600 MB Eindhoven (The Netherlands)

[†] Current address: Organic Chemistry Department (Módulo 01)  
Universidad Autónoma de Madrid  
28049 Cantoblanco (Spain)  
Fax: (+34) 91-497-3966  
<http://www.orgchem.science.ru.nl/research/andresdelaescosura/>  
E-mail: andres.delaescosura@uam.es

[#] Current address: Laboratory for Biomolecular Nanotechnology  
MESA+ Institute, University of Twente  
PO Box 207, 7500 AE Enschede (The Netherlands)  
Fax: (+31) 24-36-53393  
<http://www.orgchem.science.ru.nl/people/jeroencornelissen.php>  
E-mail: j.j.l.m.cornelissen@utwente.nl

[\*\*] We acknowledge funding from the IEF Marie Curie program of the European Union, the Chemical Council of the Netherlands Organization for Scientific Research (NWO), the EURI Scheme of the European Science Foundation (ESF), and the Royal Netherlands Academy for Arts and Sciences. We also acknowledge Paul van der Schoot and E. W. (Bert) Meijer for useful discussions, and Koen Pieterse for art work.

Supporting information for this article is available on the WWW under <http://dx.doi.org/10.1002/anie.201001702>.

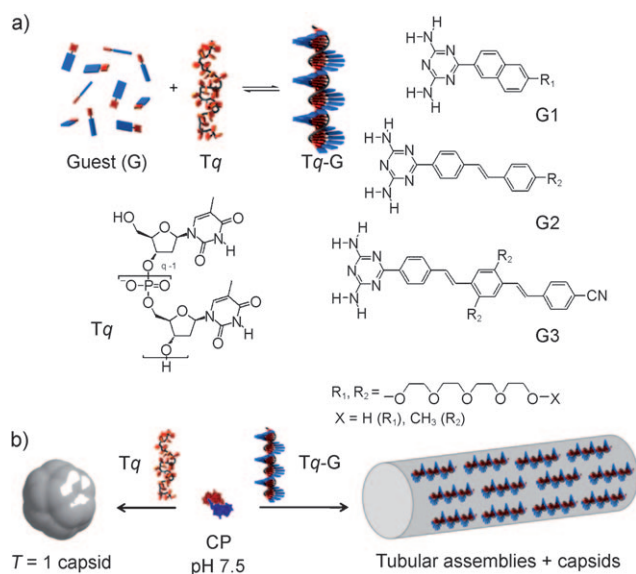


**Figure 1.** Schematic representation of a) Tq-G complexes formed between a single-stranded oligo(thymine) (Tq) (where  $q$  is the number of thymine units,  $q = 5, 10, 15, 20, 25, 30, 40$ ) and guest molecules equipped with a diaminotriazine functionality (G), and b) the assemblies formed by Tq-G in the presence of CCMV CP molecules. The arrangement of the Tq-G templates within the tubes is a tentative representation.

TEM (Figure S1b in the Supporting Information) and molecular dynamics simulations.<sup>[24]</sup>

When CP was mixed with a solution containing the T40-G1 complex in a thymine/CP ratio of 10:1, the Cotton effect of the complex was retained (Figure 2a), thus showing that G1 maintains its helical arrangement. With TEM, under uranyl acetate staining, many tubular structures of various lengths and some capsids were observed (Figure 2b). All capsids (ca. 10% of the total material under optimal conditions; see below) had mostly the same diameter, corresponding to  $T=1$  particles.<sup>[28]</sup> The tubes had a very uniform diameter of  $(19 \pm 3)$  nm (Figure 2c) and hemispherical caps similar in size as half of a  $T=1$  capsid (Figure 2d).

As a control experiment, the sample containing only CP did not show any capsids or tubes when examined by TEM (Figure S2 in the Supporting Information). The same result was obtained when G1 was mixed with CP. For mixtures of CP and T40 in a thymine/CP ratio of 10:1,  $T=1$  capsids were mainly found on the TEM grids (Figure 2e).

The order of addition of the three components (i.e., CP, T40, and G1) was found to dramatically influence the final assembly product (see experimental procedures in the Supporting Information). This result indicates a sequential two-step self-assembly process, in which the formation of T40-G1 occurs first and is followed by the nanotube assembly. The influence of the Tq length on the self-assembly process was also studied (Figure S3 in the Supporting Information). Interestingly, tubes were formed even when complexes as small as T5-G1 (ca. 2 nm in length) were used as templates.

Since the CP polymorphs were found to be stable upon dilution,<sup>[29]</sup> they were also analyzed by gel electrophoresis in agarose. Samples containing CP and T40-G1 gave an

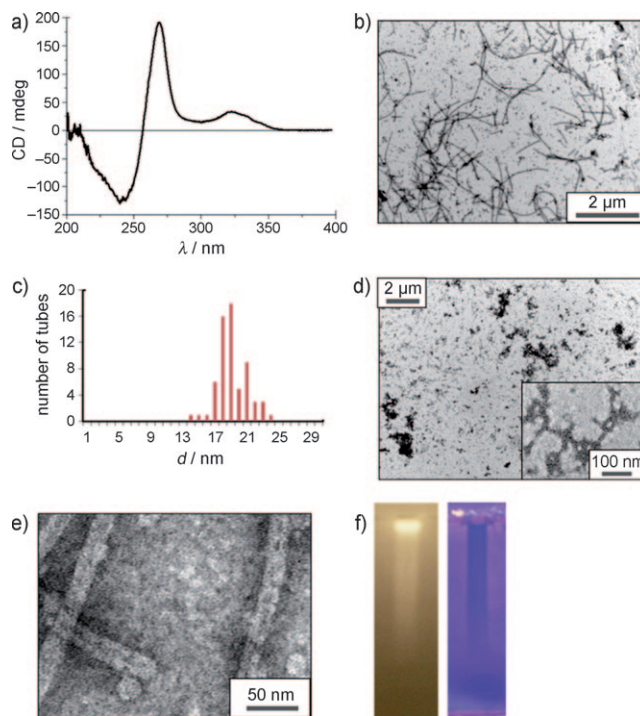


**Figure 2.** a) Circular dichroism spectrum of a mixture of T40, G1, and CP in tris(hydroxymethyl)aminomethane hydrochloride (Tris-HCl) buffer (0.1 M NaCl) at pH 7.5 and 5 °C ( $[G1] = 1$  mM,  $[T40] = 0.2$  mM, and  $[CP] = 0.04$  mM). b) TEM micrograph taken from a mixture of T40, G1, and CP under the same conditions (uranyl acetate staining). c) Size distribution diagram of tube diameters in (b). d) TEM micrograph taken from a mixture of T40 and CP under the same conditions (uranyl acetate staining). e) TEM micrograph showing the relative sizes of the end cap of a tube and a  $T=1$  capsid (uranyl acetate staining). f) Photographs of the same lane in an agarose gel, which contains T40, G1, and CP, visualized under a UV lamp (left) and by coomassie blue staining (right).

elongated band eluting towards the anode, which was attributed to the presence of tubes (Figure 2f). Control experiments were performed to ensure that this band was not an artifact (Figure S4 in the Supporting Information). The most remarkable observation from the gel electrophoresis was that the eluting band that corresponded to the tubular assemblies was clearly visible under UV illumination. There also seemed to be accumulation of light-absorbing material near the loading vessel, which may be due to very large tubes that cannot migrate into the gel. These experiments confirmed the inclusion of ssDNA-guest complexes inside the nanotubes.

In order to understand the role of T40 and G1 on the polymorphism of the coat protein assemblies, titrations were performed in which the relative concentrations of T40 and G1 with respect to the coat protein were systematically varied. All the samples in a titration series were analyzed by TEM, and the relative total areas occupied by tubes and capsids was measured for each sample (Figure 3). These measurements provided an estimate of the tendency of capsids and tubes to be assembled in each case. Every sample was prepared following the standard order of addition; that is, a solution of CP was added to the T40-G1 complex.

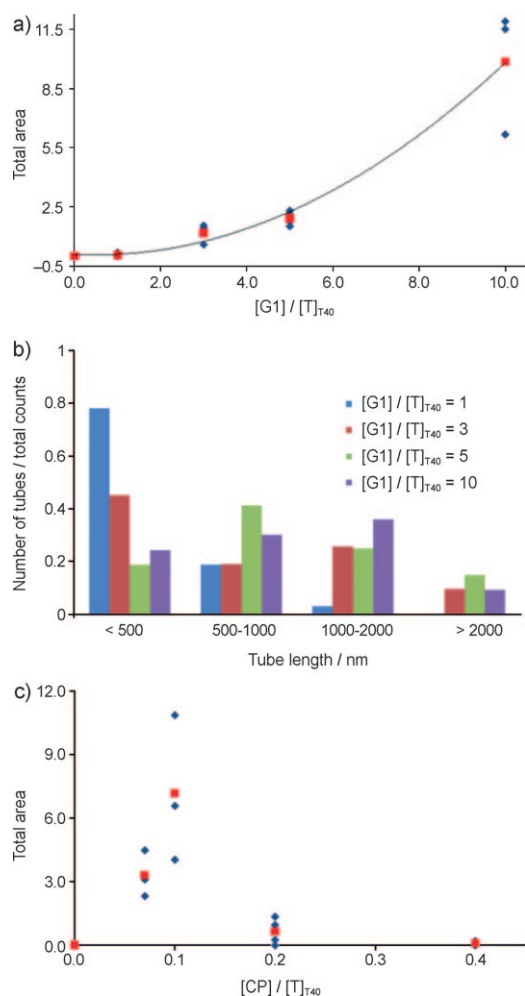


**Figure 3.** a) Plot of the ratio of total areas occupied by tubes and capsids (measured by TEM) versus the  $[G1]/[T]_{40}$  ratio, in a titration where the concentrations of CP and template binding sites were kept constant.  $[T]_{40} = 0.2$  mM and  $[CP] = 0.04$  mM. b) Histogram showing the length distribution of tubes for different  $[G1]/[T]_{40}$  assembly ratios. For  $[G1]/[T]_{40} \leq 3$ , an average of only ca. 30 tubes could be taken because of the predominant presence of capsids. For  $[G1]/[T]_{40} > 3$ , an average value of ca. 80 tubes is given. c) Plot of the ratio of total areas occupied by tubes and capsids (measured by TEM) versus  $[CP]/[T]_{40}$ , in a titration where the concentration of T40–G1 was kept constant.  $[G1] = 1$  mM and  $[T]_{40} = 0.2$  mM. Each blue data point in graphs (a) and (c) corresponds to the results from one micrograph, while the red points represent average data points obtained from three different micrographs.

A series of samples with variable amounts of G1 was first prepared, while the concentrations of CP and T40 were kept constant in a 5:1 ratio of CP and thymine units (Figure S5 in the Supporting Information). When no guest was added, only capsids were observed on the TEM grid. With each increase of the concentration of G1, more fully bound T40–G1 complexes were formed and, as a consequence, the proportion of tubes became larger (Figure 3a). The guest molecules do not only exert an influence on the quantity of the assembled nanotubes, but also on their lengths, as can be concluded from the length distribution diagram in Figure 3b. A much larger proportion of tubes shorter than 500 nm was

obtained for  $[G1]/[T]_{40} = 1$  than for higher ratios. For  $[G1]/[T]_{40} \geq 3$ , the length distribution of tubes did not change dramatically, although a slight increase in the relative amount of tubes longer than 1  $\mu$ m could be observed with an increasing  $[G1]/[T]_{40}$  ratio.

In a second series of experiments, the CP concentration was varied while keeping the T40–G1 concentration constant (Figure S6 in the Supporting Information). In the absence of CP, neither tubes nor capsids were obtained. An increase in the amount of CP led to a significant increase of assembly products. For  $[CP]/[T]_{40} < 0.2$ , tubes were the main species present (Figure 3c). At  $[CP]/[T]_{40} = 0.1$ , the proportion of tubular assemblies compared to capsids was at a maximum. This ratio corresponds to 10 binding phosphate units per CP subunit, and is remarkably close to the number of positively charged residues in the N terminus of the coat protein (9 residues).<sup>[25]</sup> At  $[CP]/[T]_{40} \geq 0.2$ , tubes were still present, but the fraction of capsids dramatically increased. The average diameter of capsids also varied slightly with the  $[CP]/[T]_{40}$  ratio (Figure S7 in the Supporting Information).

Another important issue to be evaluated is the potential of our procedure for assembling different  $\pi$ -conjugated chromophores. To this end, two other diaminotriazine derivatives G2 and G3 (Figure 1), which bear stilbene and oligo-(*p*-phenylenevinylene) moieties, respectively, were synthesized and tested for their capacity to bind to T40 and to induce hierarchical assemblies with CP. Firstly, a concentrated solution of G2 or G3 in DMSO ( $[G] = 0.04$  mM) was injected into a solution of T40 in Milli-Q water ( $[T]_{40} = 0.02$  mM). Both samples showed an induced Cotton effect in the guest absorption region, thus indicating that they bind to the T40 template. Remarkably, the Cotton effect of T40–G2 was reversed, which suggests that the helicity of this complex may be opposite to that of T40–G1 and T40–G3. The CP-containing samples were prepared in the same way as described above for experiments with G1, but for solubility reasons these samples contained 2% DMSO, and the concentrations of T40–G2 and T40–G3 were 25 times lower. CD spectra showed that the Cotton effects were retained after the samples were mixed with CP (Figure 4a), thus showing that the helical structures of these T40–G complexes remained intact. TEM studies revealed that tubes with lengths over 2  $\mu$ m had been formed (Figure 4b and Figures S8, S9 in the Supporting Information) for both T40–G complexes. The abundance of tubes on the grids was lower than for the experiments with G1 because of the lower concentration of the reagents. There were no tubes present in the absence of the guest.

The mechanism of tube formation is very intriguing. The assembly of CCMV tubular structures has been less explored than the assembly of capsids. According to the tiling theory,<sup>[30,31]</sup> CCMV tubes are thought to be rolled sheets composed of protein subunits arranged in a hexagonal lattice.<sup>[27]</sup> Very little is known, however, about the tube-assembly process. Our results seem to show that the stiffness of the polyanionic template is one of the main factors that control which polymorphs are obtained at neutral pH. The complexation of G molecules by Tq results in a rigidification of the template, which forms a supramolecular double-



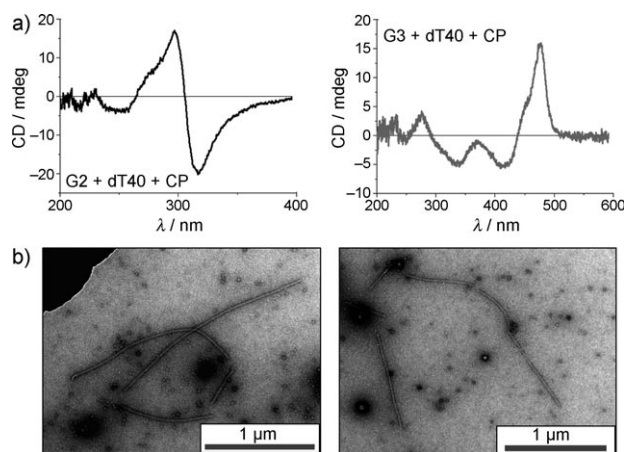


**Figure 4.** a) CD spectra of samples containing mixtures of T40, CP, and either G2 (left) or G3 (right) as guests. b) TEM micrographs of the tubular structures formed by G2 (left) and by G3 (right) in combination with T40 and CP.

stranded helix with all the negatively charged phosphate groups pointing to the exterior of the backbone. Electrostatic interactions between negative charges of the template and the positively charged CP N terminus subsequently induce the assembly of the coat proteins.

In conclusion, the hierarchical two-step self-assembly of a three-component system, that is, guest, ssDNA, and CP, can be instrumental in the encapsulation of stacking chromophores over micrometer distances. We have formulated a procedure to obtain virus protein nanotubes where any organic chromophore bearing a diaminotriazine unit could potentially be encapsulated. It is noteworthy that the tubular lengths exceed that of the DNA template by two orders of magnitude. Our studies open unique possibilities to arrange functional molecules into robust nanostructures with controlled geometry, size and position.

Received: March 22, 2010

**Keywords:** DNA structures · nanostructures · nanotubes · self-assembly · viruses

- [1] C. M. Niemeyer, *Angew. Chem.* **2001**, *113*, 4254; *Angew. Chem. Int. Ed.* **2001**, *40*, 4128.
- [2] V. M. Rotello, *J. Mater. Chem.* **2008**, *18*, 3739.
- [3] A. J. Dirks, R. J. M. Nolte, J. J. L. M. Cornelissen, *Adv. Mater.* **2008**, *20*, 3953.

- [4] S. F. M. van Dongen, H. P. M. de Hoog, R. Peters, M. Nallani, R. J. M. Nolte, J. C. M. van Hest, *Chem. Rev.* **2009**, *109*, 6212.
- [5] K. Tanaka, A. Tengeji, T. Kato, N. Toyama, M. Shionoya, *Science* **2003**, *299*, 1212.
- [6] N. C. Seeman, *Nature* **2003**, *421*, 427.
- [7] B. Samorì, G. Zuccheri, *Angew. Chem.* **2005**, *117*, 1190; *Angew. Chem. Int. Ed.* **2005**, *44*, 1166.
- [8] P. W. K. Rothemund, *Nature* **2006**, *440*, 297.
- [9] T. H. LaBean, H. Y. Li, *Nano Today* **2007**, *2*, 26.
- [10] O. I. Wilner, Y. Weizmann, R. Gill, O. Lioubashevski, R. Freeman, I. Willner, *Nat. Nanotechnol.* **2009**, *4*, 249.
- [11] M. Endo, H. Sugiyama, *ChemBioChem* **2009**, *10*, 2420.
- [12] Q. Wang, T. W. Lin, L. Tang, J. E. Johnson, M. G. Finn, *Angew. Chem.* **2002**, *114*, 477; *Angew. Chem. Int. Ed.* **2002**, *41*, 459.
- [13] S. Sen Gupta, J. Kuzelka, P. Singh, W. G. Lewis, M. Manchester, M. G. Finn, *Bioconjugate Chem.* **2005**, *16*, 1572.
- [14] T. Douglas, M. Young, *Science* **2006**, *312*, 873.
- [15] M. Uchida, M. T. Klem, M. Allen, P. Suci, M. Flenniken, E. Gillitzer, Z. Varpness, L. O. Liepold, M. Young, T. Douglas, *Adv. Mater.* **2007**, *19*, 1025.
- [16] M. Fischlechner, E. Donath, *Angew. Chem.* **2007**, *119*, 3246; *Angew. Chem. Int. Ed.* **2007**, *46*, 3184.
- [17] A. de La Escosura, R. J. M. Nolte, J. J. L. M. Cornelissen, *J. Mater. Chem.* **2009**, *19*, 2274.
- [18] C. B. Mao, D. J. Solis, B. D. Reiss, S. T. Kottmann, R. Y. Sweeney, A. Hayhurst, G. Georgiou, B. Iverson, A. M. Belcher, *Science* **2004**, *303*, 213.
- [19] K. T. Nam, D. W. Kim, P. J. Yoo, C. Y. Chiang, N. Meethong, P. T. Hammond, Y. M. Chiang, A. M. Belcher, *Science* **2006**, *312*, 885.
- [20] Z. Niu, J. Liu, L. A. Lee, M. A. Bruckman, D. Zhao, G. Koley, Q. Wang, *Nano Lett.* **2007**, *7*, 3729.
- [21] Y. S. Nam, T. Shin, H. Park, A. P. Magyar, K. Choi, G. Fantner, K. A. Nelson, A. M. Belcher, *J. Am. Chem. Soc.* **2010**, *132*, 1462.
- [22] P. G. A. Janssen, S. Jabbari-Farouji, M. Surin, X. Vila, J. C. Gielen, T. F. A. de Greef, M. R. J. Vos, P. H. H. Bomans, N. A. J. M. Sommerdijk, P. C. M. Christianen, P. Leclere, R. Lazzaroni, P. van der Schoot, E. W. Meijer, A. P. H. J. Schenning, *J. Am. Chem. Soc.* **2009**, *131*, 1222.
- [23] P. G. A. Janssen, J. L. J. van Dongen, E. W. Meijer, A. Schenning, *Chem. Eur. J.* **2009**, *15*, 352.
- [24] M. Surin, P. G. A. Janssen, R. Lazzaroni, P. Leclere, E. W. Meijer, A. Schenning, *Adv. Mater.* **2009**, *21*, 1126.
- [25] J. A. Speir, S. Munshi, G. J. Wang, T. S. Baker, J. E. Johnson, *Structure* **1995**, *3*, 63.
- [26] J. E. Johnson, J. A. Speir, *J. Mol. Biol.* **1997**, *269*, 665.
- [27] S. Mukherjee, C. M. Pfeifer, J. M. Johnson, J. Liu, A. Zlotnick, *J. Am. Chem. Soc.* **2006**, *128*, 2538.
- [28] T=1 capsids are formed by 60 coat protein subunits.
- [29] The Cotton effect was retained even under tenfold dilution, under which conditions G1 normally does not bind to T40, as shown by the absence of a CD effect if no CP is present.
- [30] R. Twarock, *Bull. Math. Biol.* **2005**, *67*, 973.
- [31] T. Keef, A. Taormina, R. Twarock, *J. Phys. Condens. Matter* **2006**, *18*, S375.